

UC Irvine

UC Irvine Previously Published Works

Title

An Investigation of South Pole NO_x Chemistry: Comparison of Model Results with ISCAT Observations

Permalink

<https://escholarship.org/uc/item/5rn0r6k7>

Journal

Geophysical Research Letters, 28(N19)

Authors

Blake, DR
Chen, G
Davis, D
[et al.](#)

Publication Date

2001

License

<https://creativecommons.org/licenses/by/4.0/> 4.0

Peer reviewed

An Investigation of South Pole HO_x Chemistry: Comparison of Model Results with ISCAT Observations

G. Chen¹, D. Davis¹, J. Crawford², J. B. Nowak¹, F. Eisele³, R. L. Mauldin III³, D. Tanner¹, M. Buhr^{1,7}, R. Shetter³, B. Lefer³, R. Arimoto⁴, A. Hogan⁵, and D. Blake⁶

Abstract. Unexpected high levels of OH and NO were recorded at the South Pole (SP) Atmospheric Research Observatory during the 1998-99 ISCAT field study. Model simulations suggest a major photochemical linkage between observed OH and NO. A detailed comparison of the observations with model predictions revealed good agreement for OH at NO levels between 120 and 380 pptv. However, the model tended to overestimate OH for NO levels < 120 pptv, while it underestimated OH at levels > 380 pptv. The reasons for these deviations appear not to involve NO directly but rather HO_x radical scavenging for the low NO conditions and additional HO_x sources for the high NO conditions. Because of the elevated levels of NO and highly activated HO_x photochemistry, the SP was found to be a strong net source of surface ozone. It is quite likely that the strong oxidizing environment found at the South Pole extends over the entire polar plateau.

1.0. Introduction

The photochemistry of near surface air at the South Pole (SP) has received minimal attention from the modeling community in past years. This most likely reflects the fact that other than O₃ and CO, little data existed to justify detailed model studies. The recent field study ISCAT (Investigation of Sulfur Chemistry in the Antarctic Troposphere) provides extensive photochemical observations so that a comprehensive modeling analysis can be carried out to investigate SP summertime photochemical processes. The ISCAT program represents an extension of the earlier SCATE program (Sulfur Chemistry in the Antarctic Troposphere Experiment) that examined sulfur chemistry at Palmer Station located on the Antarctic coast. This extension to the South Pole recognizes that the different chemical forms of sulfur found in Antarctic ice cores can serve as useful climate proxies (e.g., *Legrand, 1997* and references therein.). It also highlights the continuing need to improve our quantitative understanding of the dynamical and chemical factors influencing sulfur speciation and deposition at the SP.

Among the important chemical factors is the role played by local photochemistry in altering species before their deposition.

In this regard, the levels of the hydroxyl radical (OH) are most critical. The OH radical is now recognized as the single most important atmospheric species responsible for converting ocean-released reduced sulfur (i.e., dimethyl sulfide, DMS) to its several possible oxidized forms [*Hynes et al., 1986*].

One of the critical species that controls OH, particularly at very low temperatures, is NO (e.g., see Figure 1). Early Antarctic coastal measurements of NO during the SCATE program led to the conclusion that SP levels would probably not exceed 5 pptv [*Berresheim et al., 1998*]. Still more recent coastal field studies have tended to support this notion [*Jones et al., 2000*]. Thus, all earlier measurements would tend to minimize the importance of NO as a secondary source of OH. However, as discussed by *Davis et al.* [this issue], the 1998 ISCAT observations appear to dramatically alter this perception. The median level of NO at the SP was 225 pptv with maximum and minimum values of 600 and 15 pptv, respectively. At these NO levels, photochemical theory predicts that several other species should also be elevated, e.g., OH and HNO₃. In fact, these predictions were realized from direct observations of both species [*Mauldin et al., this issue*; and *Arimoto*, unpublished results]. Presented in this paper is a comparison of the OH model results with the observations using the new NO observations, along with other *in-situ* data, as input to the model. The SP budgets for OH and HO_x and the significance of HO_x/NO_x chemistry to O₃ formation have also been explored.

2.0. Database and Model Description

2.1. Database

This modeling study was based on the *in-situ* observations made by the ISCAT science team and by NOAA/CMDL personnel. The CMDL data included surface O₃ and total O₃ [*Oltmans et al., 1994*], CO [*Novelli et al., 1998*], and the meteorological parameters: [*Peterson, 1994*] wind direction, wind speed, temperature, dew point, and pressure. ISCAT

¹Georgia Institute of Technology, Atlanta.

²NASA Langley Research Center, Hampton, Virginia.

³National Center for Atmospheric Research, Boulder, Colorado.

⁴New Mexico State University, Carlsbad.

⁵Geochemical Sciences Division, Hanover, New Hampshire.

⁶University of California, Irvine, Irvine.

⁷Sonoma Technology, Inc., Golden, Colorado.

Copyright 2001 by the American Geophysical Union.

Paper number 2001GL013158.
0094-8267/01/2001GL013158\$05.00

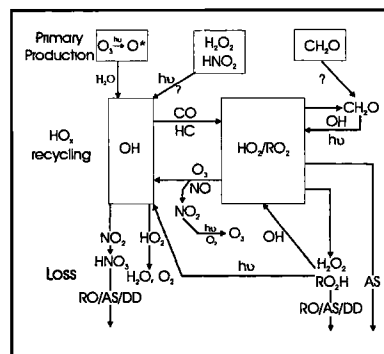


Figure 1. Simplified HO_x-NO_x-CH₄ photochemical scheme reflecting South Pole chemistry.

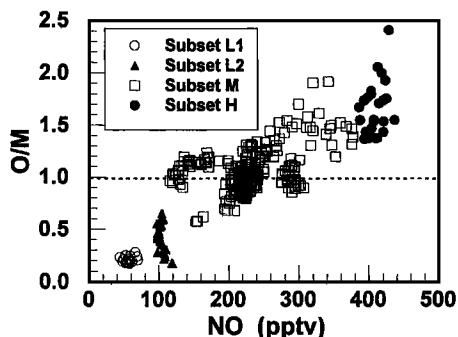


Figure 2. Ratio of observed OH to model calculated values as a function of observed NO. The division of data subsets L1, L2, M, and H was based on observed NO levels.

photochemical observations included: NO, OH, and photolysis rate coefficients for $J(\text{O}^1\text{D})$, $J(\text{NO}_2)$, $J(\text{HNO}_3)$, $J(\text{H}_2\text{O}_2)$, $J(\text{CH}_2\text{O})$, $J(\text{HONO})$, $J(\text{CH}_3\text{OOH})$, $J(\text{CH}_3\text{ONO}_2)$, and $J(\text{PAN})$.

The NO data was reported at a time resolution of 1 min. from Nov. 30, '98 to Jan. 4, '99. The modified chemiluminescence NO sensor had a 2σ detection limit (LOD) of 6 pptv. The OH data was also taken at 1 min. intervals for Dec. 12–30, '98. The OH observations were recorded using the SICIMS (select-ion chemical-ionization mass spectrometer) technique which had a nominal LOD of $\sim 5 \times 10^4$ molecule cm^{-3} based on a 5 min. integration period. The estimated total error (i.e., precision plus accuracy) was $\pm 75\%$ (2σ). At S/N ratios of 5/1 or greater, the systematic error dominated, leading to an overall uncertainty of $\sim \pm 60\%$. More detailed discussions of these measurements can be found in *Davis et al.*, *Mauldin et al.*, and *Lefer et al.* [all this issue]. In addition, there were also very limited atmospheric HNO_3 measurements (*Richard Arimoto*, unpublished results).

All data collected during the ISCAT study involved sampling from either the second floor of the NOAA operated Atmospheric Research Observatory (ARO) building or from the roof of the ARO building. The OH and NO sampling inlets at the second floor extended out 1–2 m from the building, at a height of ~ 10 m above the snow surface. All sampling inlets were mounted on the side of the ARO building facing the prevailing wind, e.g., out of the "clean air sector" ($0^\circ - 120^\circ$).

2.2. Model Description

The photochemical box model used in this study was similar to that described previously by [*Crawford et al.*, 1999]. The model assumes that all short lived species to be in photo-stationary state. The longer lived species (e.g. H_2O_2 , CH_3OOH , HNO_3 , etc) were assumed to be at steady state. Model runs were constrained by observational values of O_3 , NO, CO, H_2O , CH_4 , pressure, and temperature. For select sensitivity runs, the model was also constrained using measured values of OH. All model constraints were based on 10 min averaged data. The photolysis rate coefficients were based on *in-situ* spectrally resolved actinic flux measurements [*Lefer et al.*, this issue]. Due to the time of year (i.e., Austral summer), there was 24 hours of sunlight at the SP each day with a zenith angle of $\sim 67^\circ$. The only modulation of the J values occurred due to variations in cloud coverage and the overhead ozone column density. The estimated systematic error in the model calculations due to uncertainties in the respective "J" and "k" values has previously been evaluated using Monte Carlo calculations as $\pm 30\%$. The possible systematic error due to incompleteness in the model mechanism is being assessed in this study.

An important modification to our standard model has involved an adjustment to the first order loss rate coefficients

for soluble species. Reflecting the findings of *Davis et al.* [this issue] who characterized the SP atmospheric mixed layer as quite shallow and stratified we have reassessed the k values assigned to surface deposition and scavenging. In this case we have taken advantage of the limited measurements of HNO_3 and used this species as a surrogate for all soluble species. The first order HNO_3 loss coefficient was determined by the best fit of the model value to the observed median level, while both model OH and NO were constrained to their observed median values. However, since the HNO_3 observations were very limited, the resulting "k" values for surface loss rates must be viewed as "best estimates" only. The HNO_3 values themselves ranged from 120 to 750 pptv (*R. Arimoto*, unpublished results).

The first order loss coefficients estimated from HNO_3 ranged from 2.4×10^{-6} to $1.8 \times 10^{-5} \text{ sec}^{-1}$. For our standard model, we selected a first order "k" value near the higher end of this range, i.e., $1 \times 10^{-5} \text{ sec}^{-1}$. However, in the model's current configuration, the maximum impact on predicted OH when using other surface loss "k" values cited was only $\pm 16\%$.

3.0. Results and Discussion

3.1. OH: Observations vs. Model predictions

In the text that follows, only when both OH and NO values were recorded simultaneously was an "observation" versus "model" comparison considered. In addition, comparisons were only made when temporal variations in NO over a 20 min period were $\leq 25\%$. This filtering procedure resulted in a total of 316 independent 10 min. OH values, or $\sim 80\%$ of the total OH data.

As shown in Figure 2, in general, the agreement between model and observations was quite good, i.e., $\sim 80\%$ of the results were well within the combined uncertainties of the model and measurements. The median value for the ratio of observation to model (O/M) for all data was 1.01. This result, however, is misleading in that an inspection of the O/M ratio shows that the value for this ratio varies significantly as a function of the NO mixing ratio. As illustrated in Figure 2, O/M values are significantly less than 1 for NO levels < 120 pptv while significantly higher than unity for NO levels > 380 pptv.

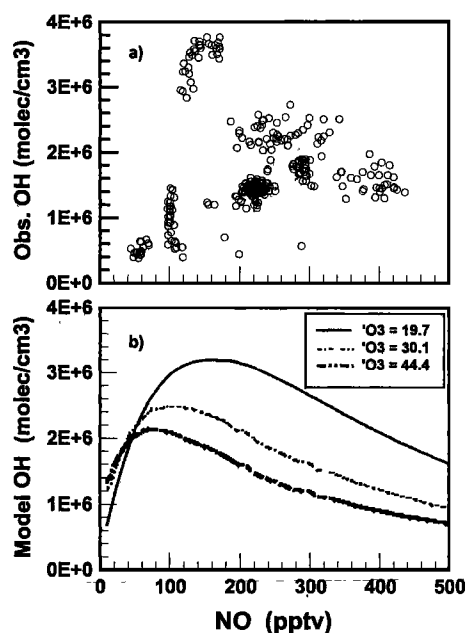


Figure 3. Observed (a) and model calculated (b) OH as a function of observed NO and O_3 levels. The three O_3 levels correspond to the 5th and 95th percentile and median values.

Table 1. South Pole OH budget

OH Source	Percent Contribution	OH Sinks	Percent Contribution
O(¹ D) + H ₂ O	6%	OH + CO	51%
HO ₂ + NO	92%	OH + CH ₄	20%
HO ₂ + O ₃	2%	OH + NO ₂	9%
		OH + O ₃	7%
		OH + H ₂	6%
		OH+CH ₂ O	4%
		Others	3%
Total	100%		100%

For mid-range values (120 to 380 pptv), the model predictions are reasonably consistent with the observations. The R² value calculated for this subset is 0.8. We have labeled this data subset as group "M".

For NO values > 380 pptv, the median O/M value is 1.6. These data have been labeled as group "H". The lowest O/M subset, labeled here as "L", has been further subdivided into groups L1 and L2. The lowest of these, L1, is made up of data primarily collected on 12/17 and reflect NO values that are shown as typically ≤ 50 pptv. The median O/M ratio for this data group is 0.21. The second "L" grouping (L2), recorded on 12/27, resulted in an estimated O/M ratio of 0.45 and corresponds to a median NO level of 100 pptv. Data groups L and H have been examined in sections 3.1.1 and 3.1.2 in greater detail, since no evidence was found for an instrument malfunction during the times of ISCAT OH sampling. Thus, data groups "H" and "L" are viewed as providing a strong indication that other factors likely influenced the SP OH which were not included in our standard model runs.

As shown in Figure 1, elevated NO promotes OH recycling through the HO₂/NO reaction. However, because of the follow-on reaction of OH with NO₂, steady increases in the level of NO do not lead to monotonic increases in OH. In fact, one typically finds that the OH concentration peaks at intermediate levels of NO as shown in Figure 3a. For the typical conditions found during ISCAT, Figure 3b shows that model predicted OH values peak at 126 pptv of NO; whereas, the experimental OH maximum, as shown in Figure 3a, indicates near max values of OH as occurring over a rather broad range of NO (i.e., 100 to 200 pptv). However, this can be largely understood in terms of the influence of varying levels of O₃. As seen in Figure 3b, where the top and bottom curves define the 5th and 95th percentile for observed O₃, the optimum NO value is seen shifting from 89 to 158 pptv, respectively. Variations of other parameters (e.g., H₂O) can also cause small shifts (i.e., ≤ 15%).

3.1.1. Detailed investigation of data groups L1 and L2.

An important atmospheric characteristic revealed from examining data subsets L1 and L2 was that very high dew points were recorded for both sampling days (i.e., -25 °C for 12/17 and -29 °C for 12/27). In fact, these were the only cloudy/foggy days during ISCAT for which both model runs and observations were available. As suggested by [Mauldin *et al.*, this issue], the environmental conditions on these two days points strongly toward the possibility that there were additional losses of HO_x radicals due to droplet scavenging. Previous studies have reported evidence of substantial HO₂ loss in clouds [Mauldin *et al.*, 1998; Cantrell *et al.*, 1996]. To simulate this loss in the current study, we introduced a first order "k" value for HO₂ with an assigned sticking coefficient, γ, of unity. This scavenging process was further assumed to be irreversible. Given the temperature and dew point on 12/17 and 12/27, we then took the supercooled water droplet size distribution as falling within the range of 5 - 10 μm and as having an estimated number density

of 5 to 15/cm³ [Austin Hogan, unpublished results]. Using the midpoint of these ranges, the resulting first order scavenging rate was estimated at $9.0 \times 10^{-3} \text{ s}^{-1}$ [Fuchs and Sutugin, 1970]. The required "k" values needed to bring the model and observations into a high level of agreement were determined to be $8.0 \times 10^{-3} \text{ s}^{-1}$ and $3.5 \times 10^{-3} \text{ s}^{-1}$ for L1 and L2, respectively. Thus, within the range of values cited for droplet parameters, a modification of the standard model was able to bring both days' predictions into reasonable agreement with the observations. The corresponding lifetimes for HO₂ are 2.1 and 4.8 minutes.

3.1.2. Detailed Investigation of Data Group H. As discussed in the above text, the group "H" appear unique in that the observed OH is substantially higher than the standard model prediction. In this context, recent polar observations indicating snow emissions of CH₂O, H₂O₂, and HONO as a possible source of HO_x radicals would appear to be quite relevant [McConnell *et al.*, 1997; Sumner and Shepson, 1999; Hutterli *et al.*, 1999; and Dibb *et al.*, 1999]. To simulate the effect of the new sources, we have carried out sensitivity runs to estimate the level of each of these species required to remove the model underestimation. Then, the estimated levels have been compared with available data from various polar sites. In the case of CH₂O, additions of only 80 pptv were found to be sufficient. Observed CH₂O levels at Summit, Greenland have ranged from 100 - 450 pptv and those at Alert, Canada from 52 - 690 pptv.

Similarly, for H₂O₂ and HONO we estimate that 190 pptv and 4 pptv, respectively, would be required. These values can be compared to summertime SP H₂O₂ measurements that have ranged from 80 to 280 pptv [McConnell *et al.*, 1997] and Summit, Greenland observations of HONO that have been found to be as high as 10 pptv [Dibb *et al.*, 1999]. Collectively, these findings would suggest that modifications to the standard model, involving the inclusion of other HO_x sources, can readily account for observed OH values exceeding those predicted using the standard model.

On the other hand, if similar levels of these new HO_x sources are applied to our group M data, the model predicted OH is increased by a factor of 1.3 to 2.5, which is significantly higher than the observed OH. By contrast, for data groups L1 and L2, the same addition of CH₂O and H₂O₂ shifts the predicted OH up by less than 20%. HONO, however, increases predicted OH by more than a factor of 2. To reconcile these discrepancies, one has to assume that the actual levels of these additional HO_x sources would to a large extent parallel NO levels, which as noted by Davis *et al.* [this issue] is strongly controlled by the atmospheric mixing depth at SP. If true, then the general trend would be one in which the levels of all four species would be significantly modulated by shifts in the mixing depth. Thus, the OH results for data groups "M" and "L" would not be expected to be as strongly influenced by the proposed additional HO_x sources as group "H". Suffice it to say, any comprehensive

Table 2. South Pole HO_x budget

HO _x Source	Percent Contribution	HO _x Sink	Percent Contribution
O(¹ D) + H ₂ O	37%	HNO ₃ + DD	52%
CH ₄	63%	HNO ₃ + OH	10%
Chemistry		HO ₂ NO ₂ + DD	22%
		HO ₂ NO ₂ + OH	6%
		OH + HO ₂	8%
		Others	2%
Total	100%		100%

understanding of this SP HO_x chemistry will require measurements of all four species.

3.2 SP OH and HO_x Photochemical Budget

As shown in Table 1, primary production of OH from the reaction O(¹D)/H₂O accounts for only 6% of the total. The major source is from the recycling reaction, NO + HO₂. Major OH sinks involve reaction with CO, CH₄, and NO₂, e.g., 51%, 20%, and 9%, respectively. The remainder is due to the reaction of OH with O₃ (7%), H₂ (6%) and CH₂O (4%).

For HO_x (shown in Table 2), the reaction O(¹D)/H₂O defines only approximately 1/3 of the total production. The largest contributor is that from CH₄ oxidation. Quite interestingly, at NO levels of 225 pptv, the CH₂O yield from CH₄ oxidation is nearly 100%. Thus, the net HO_x production from CH₄ is ~50% of the initiating reaction rate. Major loss channels for HO_x involve the long-lived nitrogen species, i.e., HNO₃ and HO₂NO₂. Approximately 90% of the HO_x lost can be accounted for by a combination of dry deposition reaction with OH.

3.3 Consequences of Intense SP HO_x Chemistry

One of the interesting consequences of the intense surface layer photochemistry at the SP is the prediction that significant net O₃ should be a result. By extension, the same statement should also apply to the entire Antarctic plateau region. This finding is quite unique relative to what is typically found at a remote surface site where NO levels are usually quite low. In the latter case one normally finds net photochemical O₃ destruction. Based on the SP observations, the predicated net photochemical production of O₃, P(O₃), is estimated to range from 1 to 6 ppbv/day (e.g., see Crawford *et al.* [this issue]). The major pathway for this formation involves the reaction HO₂/NO (see Figure 1). SP photochemical O₃ destruction ranges from 0.3 to 0.8 ppbv/day, the two most important destruction processes being OH/O₃ and OH/NO₂.

The results from the first ISCAT field study have once again demonstrated that atmospheric surprises are still to be found. Quite remarkable is the finding that the near surface atmospheric layer at SP, with greatly enhanced NO levels, produces a 24 hour average oxidizing level (i.e. OH = 1.7×10^6 molec./cm³) which rivals that of equatorial marine environments. It is also 20 times higher than the 24 hour average value estimated for Palmer Station, Antarctica [Jefferson *et al.*, 1998].

Since for most chemical species deposition to the snow surface occurs during the summer months [Bergin *et al.*, 1998], these results raise some interesting new questions about the degree to which some species might be modified before being deposited at the surface. In conjunction with growing evidence that extensive oxidative processes are also occurring within the snowpack (i.e., firn) [e.g., Sumner and Shepson *et al.*, 1999], the interpretation of the concentration levels of some climate proxy species in ice cores may need to be reexamined. These results also point to the need for new research to explore the impact from surface emissions of NO and other trace gases on near surface OH levels for other snow covered regions.

Acknowledgments. The authors would like to acknowledge that this research is partially supported by the NSF office of Polar programs and the Division of Atmospheric Chemistry through grant # OPP-9725465. The authors would also like to thank NOAA's CMDL group for making available SP O₃, CO, and meteorological data.

References

- Bergin MH, EA, Meyerson, JE Dibb, PA Mayewski, Relationship between continuous aerosol measurements and firn core chemistry over a 10-year period at the South Pole, *Geophys. Res. Lett.*, **25**, 1189-1192, 1998.
- Berresheim, H. and F. L. Eisele, Sulfur chemistry in the Antarctic Troposphere Experiment: An overview of project SCATE, *J. Geophys. Res.*, **103**, 1619-1627, 1998.
- Cantrell, C. A., R. E. Shetter, T. M. Gilpin, J. G. Calvert, F. L. Eisele, and D.J. Tanner, Peroxy radical concentrations measured and calculated from trace gas measurements in the Mauna Loa Observatory Photochemistry Experiment 2, *J. Geophys. Res.*, **101**, 14,653-14,664, 1996.
- Crawford, J. D. Davis, J. Olson, G. Chen, S. Liu, G. Gregory, J. Barrick, G. Sachse, S. Sandholm, B. Heikes, H. Singh, and D. Blake, Assessment of upper tropospheric HO_x sources over the tropical Pacific based on NASA GTE/PEM data: Net effect on HO_x and other photochemical parameters, *J. Geophys. Res.*, **104**, 16255-16273, 1999.
- Crawford, J. H., D. Davis, G. Chen, M. Buhr, R. Shetter, B. Lefler, A. Hogan, R. Arimoto, S. Oltmans, and R. Weller, Evidence for photochemical production of ozone at the South Pole surface, this issue.
- Davis, D., et al., Unexpected high levels of tropospheric NO at the South Pole: Observations and chemical consequences, this issue.
- Dibb, J. E. et al. Photochemistry in snow: Recent findings in Greenland and Michigan and their implications for Arctic tropospheric chemistry, AGU Fall meeting, 1999.
- Fuchs, N. A. and A. G. Sutugin, Highly Dispersed Aerosols, Ann Arbor Science Publishers, Ann Arbor, Michigan, 1970.
- Hynes, AJ, P. Wine, and DH Semmes, Kinetics and mechanism of OH reactions with organic sulfides, *J. Phys. Chem.*, **90**, 4148-4156, 1986.
- Hutterli, M. A., Rothlisberger, R., Bales, R. C., Atmosphere-to-snow-to-firn transfer studies of HCHO at Summit, Greenland, *Geophys. Res. Lett.*, **26**, 1691-1694, 1999.
- Jefferson, A., D. J. Tanner, F. L. Eisele, D. D. Davis, G. Chen, J. Crawford, J.W. Huey, A. L. Torres, and H. Berresheim, OH photochemistry and methane sulfonic acid formation in the coastal Antarctic boundary layer, *J. Geophys. Res.*, **103**, 1647-1656, 1998.
- Jones, A. E., R. Weller, E. W. Wolff, and H. W. Jacobi, Speciation and rate of photochemical NO and NO₂ production in Antarctic snow, *Geophys. Res. Lett.*, **27**, 345-348, 2000.
- Lefler, B., S. Hall, L. Cinquni, and R. Shetter, Photolysis frequency measurements at the South Pole during ISCAT-98, this issue.
- Legrand, M., Ice-core records of atmospheric sulphur, *Philos T Roy Soc B*, **352**, 241-250, 1997.
- Mauldin, R. L. III, G. J. Frost, G. Chen, D. J. Tanner, A. S. H. Prevot, D. D. Davis, and F. L. Eisele, OH Measurements during the First Aerosol Characterization Experiment (ACE 1): Observations and model comparisons, *J. Geophys. Res.*, **103**, 16,713-16,729, 1998.
- Mauldin, R. L. III, F.L. Eisele, D.J. Tanner, E. Kosciuch, R. Shetter, B. Lefler, S.R. Hall, J.B. Nowak, M. Buhr, G. Chen, P. Wang, and D. Davis, Measurements of OH, H₂SO₄, and MSA at the South Pole During ISCAT, this issue.
- McConnell, J. R., R. C. Bales, R. W. Stewart, A. M. Thompson, M. R. Albert and R. Ramos, Physically based modeling of atmosphere-to-snow-to-firn transfer of hydrogen peroxide at South Pole, *J. Geophys. Res.*, **103**, 10,561-10,570, 1997.
- Ridley, B. A. and L. C. Howlett, An instrument for nitric oxide measurements in the stratosphere, *Rev. Sci. Instrum.*, **45**, 742, 1974.
- Novelli PC, KA Masarie, PM Lang PM, Distributions and recent changes of carbon monoxide in the lower troposphere, *J. Geophys. Res.*, **103**, 19,015-19,033, 1998.
- Oltmans, S. J. and H. Levy II, Surface ozone measurements from a global network, *Atmos. Environ.*, **28**, 9-24, 1994.
- Peterson, James T, Climate Monitoring & Diagnostics Laboratory #22 Summary Report, 1993-1994, US Dept. of Commerce, NOAA, 325 Broadway R/CMDL, Boulder, CO 80305, December, 1994
- Sumner, A. L., and P. B. Shepson, Snowpack production of formaldehyde and its effect on the Arctic troposphere, *Nature*, **398**, 230-233, 1999.

G. Chen, School of Earth and Atmospheric Sciences, Georgia Institute of Technology, Atlanta, GA 30332. (gaochen@eas.gatech.edu)

(Received March 9, 2001; revised July 7, 2001; accepted July 7, 2001.)